Studies in Science of Science | ISSN: 1003-2053
https://doi.org/10.5281/zenodo.18586214

Fioria Vitifolia Mediated Cuo Nanoparticles: Characterization, Biological Applications and In-Vivo Studies in Wistar Rats

Bhuvaneswari S [1], Suresh V [2*], Muthukumaran G [2], Deepan Natarajan[2], Srinivas. V[2],
[1, 2] Department of Pharmacology, JKKMMRFs- Annai JKK Sampoorani Ammal College of Pharmacy, Komaraplayam, Namakkal-638183, Tamil Nadu, India. Affiliated by The Tamil Nadu, Dr.M.G.R. Medical University, Chennai, TamilNadu, India.

Received: Jan 01, 2026 **Accepted:** Feb 01, 2026 **Published:** Feb 10, 2026

ABSTRACT:

Nanotechnology, the science of manipulating materials at the nanoscale (1–100 nm), has emerged as a transformative field with vast biomedical potential. Among various nanoparticles, copper oxide nanoparticles (CuO NPs) have attracted attention for their remarkable physicochemical and biological properties. The present study focuses on the green synthesis of CuO nanoparticles using Fioria vitifolia leaf extract as a natural reducing and stabilizing agent. Phytochemical screening of the ethanolic extract revealed the presence of alkaloids, tannins, flavonoids, triterpenoids, and phenolic compounds responsible for nanoparticle formation. The synthesized FV-CuO NPs were characterized using FTIR, XRD, SEM, EDX, TEM, UV–Vis spectroscopy, Tauc's plot, and zeta potential analysis. FTIR confirmed the functional groups involved in stabilization, while XRD indicated high crystallinity and purity. SEM and TEM analyses revealed uniform nanoscale morphology, and EDX confirmed the elemental composition. The optical band gap determined by Tauc's plot validated the nanosized nature, while zeta potential analysis confirmed excellent colloidal stability. Biological evaluations demonstrated potent antimicrobial, antioxidant, and anti-inflammatory activities. Furthermore, the MTT assay on the MDA-MB-231 (triple- negative breast cancer) cell line revealed a dose-dependent cytotoxic effect, highlighting the anticancer potential of FV-CuO NPs. Biochemical, haematological, and histopathological assessments supported their safety and therapeutic relevance. Overall, the study establishes Fioria vitifolia-mediated CuO nanoparticles as promising eco-friendly nanomaterials with significant biomedical applications.

Keywords: Copper oxide, Nanotechnology, Fioria vitifolia and nanoparticles.

1. INTRODUCTION:

Medicinal plants are naturally occurring species whose various parts—such as leaves, roots, bark, fruits, seeds, or flowers—harbor bioactive compounds that can be utilized for the prevention, management, or treatment of diseases in both humans and animals. These plants have been fundamental to traditional healing practices for millennia, underpinning systems like Ayurveda, Siddha, Unani, Traditional Chinese Medicine, and numerous indigenous healing traditions worldwide[1].The therapeutic potential of these plants is attributed to their diverse array of phytochemicals, including alkaloids, flavonoids, tannins, terpenoids, glycosides, saponins, and phenolic compounds, which exhibit a multitude of biological activities such as anti-inflammatory, antioxidant, antimicrobial, anticancer, antidiabetic, and cardioprotective effects. In contemporary medicine, medicinal plants remain crucial, with a significant portion of modern pharmaceuticals being either directly derived from these plants or chemically modified versions of plant-based compounds[2-3].The World Health Organization (WHO) indicates that approximately 80% of the global population depends on herbal medicines for various aspects of primary healthcare, highlighting their accessibility, cultural

significance, and therapeutic efficacy. Recent advancements in Phytochemistry, molecular biology, pharmacology, and biotechnology have further propelled research into medicinal plants, facilitating the discovery of new therapeutic agents and providing scientific validation for traditional herbal remedies[4].

Nanomaterials are developed, characterized, investigated, and utilized within the fields of nanotechnology and nanoscience to address the increasing demands of society[5].Advancements in nanoscience have broadened the scope of various fields by necessitating modifications in attributes, shape, size, structure, functionality, and alignment. This progress is evident across a range of disciplines, including optics, electronics, mechanics, biological sciences, food technology, space exploration, drug delivery systems, energy science, gene transfer, optoelectronic devices, catalysis, and photo-electrochemical devices[6]. Nanoparticles can enhance their bacteriostatic properties either independently or through synergistic interactions with other substances[7]. The recognition of the beneficial properties of phytochemicals has spurred researchers to explore additional applications. In 1959, Richard Feynman introduced the concept of manipulating individual atoms and molecules in his seminal work, "There's plenty of room at the bottom," which laid the groundwork for the emerging field of nanotechnology. More recently, an innovative interdisciplinary approach has emerged that focuses on synthesizing nanomaterials from phytochemicals found in plant extracts. This method is not only more environmentally friendly than traditional techniques but also eliminates the need for hazardous chemicals[8, 9].

Plant-mediated nanomaterials synthesis constitutes a facet of green synthesis that utilizes phytochemical compounds found in plant extracts as both stabilizing and reducing agents[10].The method of synthesis, along with the specific parameters employed during the production of nanomaterials, significantly influences the resulting geometries of these materials. This approach typically adopts a bottom-up strategy, utilizing various biotechnological techniques to derive materials from plant extracts. In contrast to traditional synthesis methods, which often involve hazardous chemicals, pose biological risks, and require substantial energy, plant-mediated synthesis is regarded as a more environmentally friendly and less toxic alternative[11-12].

Numerous established methods for synthesizing copper oxide nanoparticles (CuO NPs) include chemical precipitation, sol-gel processes, hydrothermal techniques, and biological approaches[13].Traditional chemical and physical synthesis methods often rely on toxic reagents and intricate procedures, highlighting the need for safer alternatives[11]. Utilizing plant extracts for the green synthesis of CuO NPs offers a sustainable solution, as the phytochemicals in these extracts serve as both reducing and stabilizing agents. This eco-friendly approach not only eliminates harmful chemicals but also involves complex biochemical interactions that facilitate the transformation of metal precursors into nanoparticles[14]. The biomolecules present help control the size and morphology of the NPs while preventing agglomeration, ultimately enhancing their functional properties. With a larger surface area, CuO NPs demonstrate effective photocatalytic activity, efficiently degrading complex organic pollutants into less harmful by-products through advanced oxidation processes.

Many research has shown that these nanoparticles can generate reactive oxygen species (ROS) that interact with pollutant molecules, leading to their mineralization[15]. The exceeding research demonstrated that CuO NPs has anti-microbial activity by the process primarily entails the disruption of the microbial cell wall, coupled with the production of reactive oxygen species (ROS) that lead to oxidative stress within the microbial cell[16].

Therefore, this study aims to fill a notable research gap by exploring the use of F. vitifolia, a plant not previously recognized for its ability to synthesize nanoparticles, in the development of an environmentally friendly method for producing silver nanoparticles

(CuONPs). We propose that the phytochemicals present in F. vitifolia can effectively reduce copperoxide and stabilize the resulting nanoparticles, thereby reducing environmental impact while also utilized the plant's therapeutic properties. Although the medicinal attributes of F. vitifolia have not been thoroughly investigated, it is thought to exhibit anti-inflammatory, analgesic, and antioxidant effects.Our research utilized an environmentally friendly method for synthesizing zinc oxide nanoparticles (ZnO NPs) using leaf extract from Fioria vitifolia Linn. The study aimed to produce these nanoparticles and assess their characteristics through various techniques, including transmission electron microscopy (TEM), scanning electron microscopy with energy-dispersive X-ray spectroscopy (SEM-EDX), Fourier-transform infrared spectroscopy (FTIR), X-ray diffraction (XRD), and UV-visible spectroscopy. Additionally, we investigated the biological applications of the synthesized nanoparticles, focusing on cytotoxicity assays with MDA-MB-231 cancer cells, as well as their antibacterial and anti-biofilm properties.

1.1. PLANT PROFILE: [17]

Common name: Hibiscus vitifolius
Kingdom: Plantae
Clade:Tracheophytes
Clade:Angiosprems
Clade: Eudicots
Clade:Rosids
Order:Malvales
Family:Malvaceae
Genus: Hibiscus
Species:H. vitifolius



Fig. no: 1. Fioriavitifolia (L.)

1.2. DISCRIPTION AND MEDICINAL USES:

Fioriavitifolia (L.) Mattei, belonging to the Malvaceae family, is a perennial herbaceous plant found extensively in the tropical regions of Asia and Africa[18]. This plant is well-regarded for its medicinal properties and is commonly utilized in traditional medicine to address various health issues, including inflammation, wounds, fever, and skin infections. Fioriavitifolia is distinguished by its soft, velvety leaves, flowers that range from pink to purple, and a fibrous stem. It is known to harbor a variety of phytochemicals, such as flavonoids, tannins, saponins, phenolic compounds, and alkaloids[19]. These bioactive compounds are responsible for its recognized antioxidant, anti-inflammatory[20], antimicrobial[21] and cytoprotective effects[22], positioning the species as a valuable subject for pharmacological research. Recent investigations have underscored the efficacy of Fioriavitifolia extracts in scavenging free radicals and modulating inflammatory pathways, thereby reinforcing its traditional uses in medicine.

2. MATERIALS AND METHODS:

2.1. Materials:

Fioriavitifolia plant leaves were gathered from Chithode in the Erode District, with initial plant identification facilitated by Botany researchers. Copper oxide nanoparticles (CuO NPs) and ethanol were procured from Sigma Aldrich (AR grade), and the study utilized a Soxhlet apparatus, double-distilled water, a digital centrifuge, a microtiter plate, the MDA-MB-231 cell line, a microscope, a CO2 incubator, and a gyratory shaker for various experimental procedures.

2.2. Prepare of Extraction:

The dried leaves of Fioriavitifolia were crushed into a powder and extracted using Soxhlet using petroleum ether and ethanol. The resultant extracts were concentrated at 45°C with a rotating vacuum evaporator until all solvents were evaporated, yielding a semisolid

mass of crude extracts. These extracts were then collected and dried in a hot air dryer at 52°C to yield powdered forms. The various extracts' yields will be examined for preliminary evaluation and pharmacological research related to in-vivo anti-diabetic effectiveness[23].

2.3. Phytochemical screening:

The Ethanolic extract of the plant Fioriavitifolia leaves was investigated top preliminary phytochemical studies[24].

2.4. Preparation and characterization of Copper oxide nanoparticles:

Characterization of FV CuO NPs:

A small amount of the synthesized FV-CuO nanoparticles (NPs) was combined with a suitable matrix, such as Potassium Bromide (KBr), to create a pellet. This pellet was subsequently positioned in the sample holder of the FTIR Spectrometer. After calibrating the instrument, the sample was scanned across a wavelength range of 4000 to 400 cm^{-1}. The resulting spectrum revealed absorption peaks that corresponded to various functional groups found in the FV-CuO NPs, as well as the phytochemicals that served as stabilizing or capping agents. Analyzing these peaks allowed for the identification of the chemical bonds and functional groups involved in the formation and stabilization of the nanoparticles[25].

XRD- X-Ray Diffraction Analysis:

X-Ray Diffraction (XRD) analysis was conducted to assess the crystalline structure, phase purity, and crystallite size of the synthesized FV-CuO nanoparticles (NPs). The dried FV-CuO NPs powder was placed in a sample holder and analysed using a D8 Advanced Powder X-Ray diffractometer. Diffraction patterns were recorded over a 2θ range of 10° to 70°, with a scanning speed of 10° per minute and a step size of 0.02°. The instrument operated at a voltage of 40 kV and a current of 50 mA[25].

The obtained diffraction peaks correspond to the characteristic reflections of crystalline CuO, confirming the formation of Copper Oxide nanoparticles. The average crystallite size (D) of the FV CuO NPs was calculated using Debye-Scherrer equation: [26-27]

$$D=k\lambda/\beta\cos\theta$$

Where,
k is the Shape factor(0.9)
ʎ is the X-Ray wavelength (1.541Å for Cu kα radiation)
β is the full width at half maximum (FWHM) of the diffraction Peak and
θ is the Bragg's diffraction angle

UV-Visible Spectroscopic Analysis

The formation and stability of Fioria vitifolia-mediated CuO nanoparticles (FV CuO NPs) were validated through UV-Visible Spectroscopy. Optical measurements were conducted over a wavelength range of 200-700 nm using a Jasco Double-beam spectrophotometer with a resolution of 1 nm. The emergence of a distinct absorption peak within this spectrum confirmed the successful synthesis of CuO nanoparticles. Furthermore, the intensity and position of this absorption peak were influenced by factors such as particle size, shape, and dispersion quality[21].

Tauc's Plot

The optical band gap energy (E_g) of the biosynthesized CuO nanoparticles was estimated using the Tauc's plot method. The analysis was performed by plotting $[F(R_\infty)hv]^2$ against the photon energy(hv), where $F(R_\infty)$ represents the absorption coefficient obtained from the diffuse reflectance data, and hv is the photon energy. The optical band gap (E_g) value was determined by extrapolating the linear portion of the plot to the x-axis, where $(F(R_\infty)hv)^2$-0. The obtained band gap value provides insights into the electronic transition and optical properties of the synthesized CuO nanoparticles[28].

SEM and EDX- Scanning Electron Microscopy and Energy Dispersive X-Ray Analysis

The synthesized nanoparticles' surface morphology and elemental composition were analyzed through Scanning Electron Microscopy (SEM) combined with Energy Dispersive X-ray (EDX) analysis. The SEM was conducted using a ZEISS Sigma Instrument at an accelerating voltage of 15 kV. A small sample of the Fioria vitifolia-mediated CuO nanoparticles (FV CuO NPs) was placed on a clean, conductive substrate, such as a silicon wafer or copper grid, and allowed to dry thoroughly to avoid particle aggregation. For non-conductive samples, a thin gold or carbon coating was applied to improve surface conductivity and enhance image clarity. The high-resolution SEM images yielded valuable information regarding the morphology, particle size, and surface texture of the FV CuO NPs[28].

The elemental composition of the nanoparticles was further analysed using EDX, integrated with the same SEM setup. The Electron beam interaction with the sample generated characteristic X-rays, which were detected to determine the qualitative and quantitative elemental composition of the FV CuO NPs. This combined SEM-EDX approach confirmed the presence of copper and oxygen as the main constituents, verifying the successful synthesis of CuO nanoparticles and their elemental purity[29].

TEM:

The morphology and crystalline properties of the synthesized FV-CuO nanoparticles (FV-CuO NPs) were analysed using a Transmission Electron Microscope (FEI Tecnai T20) at an accelerating voltage of 200 kV. To prevent agglomeration, a small amount of the nanoparticles was dispersed in distilled water and subjected to ultra-sonication for five minutes. A drop of this well-dispersed suspension was then placed on a carbon-coated copper grid (300 mesh) and allowed to dry completely in ambient conditions. After drying, the grid was mounted on the sample holder for high-resolution imaging under the TEM. Additionally, Selected Area Electron Diffraction (SAED) patterns were recorded to assess the crystalline nature and phase purity of the FV-CuO NPs. The particle size distribution was further analysed from the TEM micrographs using Image J software[30-31].

Zeta potential:

The surface charge and colloidal stability of the synthesized FV-CuO nanoparticles (FV-CuO NPs) were assessed using a Zeta Potential Analyser. A small quantity of the nanoparticles was dispersed in double distilled water and subjected to ultra-sonication for five minutes to achieve a homogeneous suspension. Measurements were conducted at room temperature with disposable folded capillary cells. The zeta potential was derived from the electrophoretic mobility of the particles in an electric field, as measured by laser Doppler velocimetry. The resulting zeta potential value indicates the surface charge of the FV-CuO NPs, offering valuable insights into their colloidal stability and dispersion characteristics in aqueous environments[32-33].

2.4. Pharmacological Evaluation of FV- mediated CuO NPs:

Antioxidant Activity [34, 35]

DPPH Free Radical Scavenging Assay

The antioxidant properties of the synthesized FV-CuO nanoparticles (FV-CuO NPs) were evaluated using the DPPH free radical scavenging assay. Methanol served as the solvent for the entire procedure. A fresh 0.1 mM DPPH solution was prepared in methanol and stored in the dark to avoid degradation. Stock solutions of FV-CuO NPs were created at a concentration of 10 mg/ml and subsequently diluted to achieve working concentrations of 20, 40, 60, 80, and 100 µg/ml. For the assay, 1 ml of the DPPH solution was combined with 1 ml of FV-CuO NPs at each concentration, thoroughly mixed, and incubated in the dark at room temperature (23±2°C) for 30 minutes. Ascorbic acid (0.1 mM) in methanol was used as a standard antioxidant control, while methanol alone served as the blank. After incubation, the

absorbance of each solution was measured at 517 nm using a Shimadzu UV-1800 UV-Vis spectrophotometer.

The percentage of DPPH radical scavenging (Inhibition) was calculated using the formula.

$$\text{Scavenging Activity}(\%) = (\text{A control} - \text{A sample} \div \text{A control}) \times 100$$

Where,

A control, is the absorbance of the DPPH solution without sample

A sample, is the absorbance in the presence of FV-CuO NPs

A decrease in absorbance indicates higher free radical scavenging activity of the sample.

The concentration of the sample required to inhibit 50% of the DPPH radicals (IC50) was determined from the graph plotted between the percentage of inhibition and sample concentration.

ABTS Radical Scavenging Test [36]

The ABTS radical scavenging activity was evaluated through a modified ABTS radical cation decolorization assay. A 7 mM stock solution of ABTS was prepared in deionized water and combined with 2.45 mM potassium persulfate (K2S2O8) to produce the ABTS free radical cation. This mixture was allowed to stand in the dark at room temperature for 12 to 16 hours prior to use. The resulting ABTS free radical solution was then diluted with ethanol to achieve an absorbance of 0.70 ± 0.02 at 734 nm. For the scavenging assay, 0.3 ml of the ABTS working solution was combined with 1.7 ml of phosphate buffer (pH 7.4) and varying concentrations of the sample extract (ranging from 10 to 50 µg/ml) to reach a final volume of 2 ml. The mixture was incubated in the dark at 25°C for 20 minutes, after which the absorbance was measured at 734 nm using a UV-Vis spectrophotometer, with phosphate buffer serving as the blank and a control prepared without the sample extract.

The radical scavenging activity (%) was calculated using the following formula:

$$\text{Scavenging Activity}(\%) = (\text{A control} - \text{A sample} \div \text{A control}) \times 100$$

The IC 50 value, representing the concentration of the extract required to scavenge 50% of the ABTS radicals, was obtained by plotting the percentage inhibition against sample concentration.

Anti-inflammatory Assay [37]

The anti-inflammatory properties of FV CuO nanoparticles were assessed through the protein denaturation method, utilizing Bovine Serum Albumin (BSA) as a model protein. A reaction mixture was created by combining 1 ml of a 1% BSA solution with varying concentrations of FV CuO nanoparticles, ranging from 20 to 100 µg/ml. The pH of this mixture was adjusted to 6.3 using 1N HCl. Following this, the samples were incubated at 37°C for 20 minutes and subsequently heated to 70°C for 5 minutes to promote protein denaturation. After the heating process, the samples were allowed to cool to room temperature.

Control-BSA solution

Standard-Diclofenac sodium (at equivalent concentrations)

The percentage inhibition of protein denaturation was calculated using the following equation:

$$\text{Inhibition } (\%) = 1 - (\text{A sample}/\text{A control}) \times 100$$

Where, A sample and A control represent the absorbance values of the test and control samples, respectively.

The IC50 value (concentration required to inhibit 50% of protein denaturation) was determined by plotting percentage inhibition against sample concentration. Higher inhibition indicates better anti-inflammatory activity of the FV CuO NPs, likely due to their ability to stabilize protein structure and prevent heat induced denaturation.

Antimicrobial Assay [38]

Antibacterial and Antifungal Activity of FV-CuO Nanoparticles

The antimicrobial potential of the synthesized FV-CuO nanoparticles (FV-CuO NPs) was evaluated against five pathogenic microorganisms, including two Gram-Negative Bacteria- Pseudomonas aeruginosa (ATCC 27853) and Proteus vulgaris (ATCC 6380) and two Gram Positive Bacteria-Staphylococcus aureus (MTCC 737) and Enterococcus faecalis (ATCC 15753). In addition, the antifungal activity was tested against Candida albicans (ATCC 10231). All the microbial strains were obtained from the Department of Oral and Clinical Pathology, Saveetha Dental College, Saveetha University, Tamil Nadu, India[39].

Each bacterial strain was cultured on nutrient agar slants and incubated at 37° C for 24 hours to obtain fresh colonies. The fungal strain (C.albicans) was cultured on potato dextrose agar (PDA) under the same conditions. For the antimicrobial assay, 24-hour old bacterial cultures were inoculated into nutrient broth and incubated at 37° C for 24 hours with gentle shaking to ensure uniform growth.

The agar well diffusion method was employed to determine the antimicrobial efficacy of FV-CuO NP. Sterile nutrient agar plates were swabbed uniformly with each bacterial culture to form a bacterial lawn, and wells (6mm in diameter) were aseptically punched into the agar using a sterile cork borer. Each well was loaded with 50µg/ml and 100 µg/ml of FV-CuO NPs suspension. The plates were then incubated at 37°C for 24h. After incubation, the zones of inhibition (Clear regions surrounding the wells) were measured in millimetres to assess antibacterial activity.

For the antifungal assay, C.albicans was similarly inoculated on PDA plates and wells were loaded with 50µg/ml and 100 µg/ml of FV-CuO NPs suspension. Plates were inoculated at 37°C for 48 h and the resulting inhibition zones were recorded. Amoxicillin served as the standard Antibiotic for bacterial strains, while Fluconazole was used as the reference antifungal agent.

Anticancer Assay:

MTT Assay on MDA-MB-231 cell line:

The MTT assay (3-(4, 5 dimethylthiazol-2-yl)-2-5-diphenyltetrazolium bromide-yellow coloured, water soluble) is a colorimetric assay commonly used to evaluate cell metabolic activity which correlates with cell viability and proliferation. It is widely employed in cytotoxicity studies of drug candidates, nanoparticles and natural extracts on cancer cell lines such as MDA-MB-231, a triple negative human breast cancer cell line.

MTT is reduced by mitochondrial dehydrogenases in viable cells to form insoluble purple formazan crystals, which are then solubilised in DMSO or a suitable solvent. The absorbance of the resulting solution is measured at 570nm, and the intensity correlates with the number of viable cells [40].

MDA-MB-231 human breast cancer cells were maintained in complete DMEM (10% FBS, 1% Penicillin-streptomycin) at 37°C and 5% CO2. For the MTT assay, cells were seeded in 96-well plates at 1.0×10^4 cells/ well and allowed to adhere 16-20h. Medium was then replaced with fresh medium containing FV-CuO NPs at 5, 10, 15 and 20µg/ml. Control Cells received vehicle only. After 24h exposure, 20µl of MTT solution (5mg/ml in PBS) was added per well and plates were incubated for 4h to allow formation of formazan crystals. Formazan crystals were dissolved in 100µl DMSO per well with gentle shaking for 10-15 min and absorbance measured at 570nm with 630nm reference.

All treatments were performed in triplicate and values reported as mean ± SD. % cell viability was calculated as (mean absorbance of treated / mean absorbance of control)× 100.

IC 50 values were derived by non-linear regression of concentration response curves; statistical comparisons used one way ANOVA with Dunnett's test $p< 0.05$[40]

2.5. Experimental Design

All animals are approved by CCPSEA under IAEC Committee the Approval no: (JKKMMRAFCP/IAEC/2025/002) the study consisted of five groups subjected to different treatments and evaluation parameters. Group I served as the control and was observed for 14 days, during which body weight and haematological parameters were assessed. Group II received a 5 µg/ml dose for 14 days, with evaluations focused on blood chemistry as well as liver and kidney function tests. Group III was treated with 10 µg/ml for 7 days, and oxidative stress markers were measured. Group IV received 15 µg/ml for 7 days, with histopathological examinations conducted. Finally, Group V was administered 20 µg/ml for 21 days to assess therapeutic efficacy.

2.6. Biochemical Parameters

Body Weight:

All the rats were weighed from the beginning to the 15th day of the study. Average increase in body weight on the 15th day was determined.

Haematological Parameters:

After 14 days, the rats were euthanized under anaesthesia with Thiopental sodium (2.5 mg i.p), and blood samples were collected. The retro-orbital plexus method was employed for blood extraction to evaluate haematological and serum biochemical parameters. A cell analyser was utilized to measure haematological parameters, including red blood cells (RBC), white blood cells (WBC), packed cell volume (PCV), haemoglobin, and platelets. The isolated serum underwent analysis for liver function tests, specifically ALT (Alanine Aminotransferase), AST (Aspartate Aminotransferase), ALP (Alkaline Phosphatase), bilirubin, as well as kidney function tests, which included urea, creatinine, and blood urea nitrogen (BUN), Nitrogen, and Antioxidant parameters like SOD-Superoxide dismutase, CAT-Catalase, MDA- Malondialdehyde, GSH-Reduced Glutathione.

2.7. Histopathological studies:

Histopathological examination will involve the analysis of liver and kidney sections to assess potential toxicity or pathological alterations. For the liver tissue, homogenate was promptly extracted and washed with cold 0.9% NaCl before being homogenized in a 10% Tris-HCl buffer (0.1 mol/L, pH 7.4). The mixture was then centrifuged at 1500 rpm for 15 minutes at 4°C, and the resulting supernatant was utilized to evaluate oxidative stress markers.

2.8. Statistical analysis:

Statistical studies were conducted using ANOVA, followed by Tukey's post hoc test to assess the data. The results will be presented as mean values with standard deviation (SD), and statistical significance will be determined at a level of $p < 0.05$.

3. Result and Discussion:

3.1. Results:

3.1.1. Preliminary Phytochemical Analysis of FV Ethanolic Extract

The extraction of Fioria vitifolia leaf using 80% ethanol as the solvent resulted in a yield of 8.95%. The extract exhibited a viscous, dark brownish-green hue, suggesting a significant concentration of phytoconstituents present in the material.

The analysis indicates that the phytoconstituents identified are predominantly terpenoids, which are present in high concentrations. Preliminary phytochemical investigations of the ethanolic extract from Fioria vitifolia leaves revealed significant levels of alkaloids, tannins, saponins, triterpenoids, flavonoids, proteins, and phenolic compounds. In contrast, glycosides and carbohydrates were found in lower concentrations, while steroids were either present in very minimal amounts or absent altogether.

3.1.2. Characterization of FV CuO NPs

3.1.2. A). FT-IR Spectroscopic Analysis

The FTIR spectrum of green synthesized FV CuO nanoparticles, as shown in Fig 7.2 a, reveals significant absorption bands at 3450 cm^{-1}, 1614 cm^{-1}, 1384 cm^{-1}, 1021 cm^{-1}, 835 cm^{-1}, 598 cm^{-1}, and 527 cm^{-1}. The prominent band at 3450 cm^{-1} is associated with the stretching vibrations of –OH groups from adsorbed water and phenolic compounds derived from plant metabolites. Meanwhile, the peaks at 1614 cm^{-1} and 1384 cm^{-1} correspond to the C=O and C-N stretching vibrations of amides and aromatic substances. Additionally, the bands observed below 600 cm^{-1} are indicative of Cu-O stretching vibrations, thereby confirming the successful synthesis of CuO nanoparticles.

3.1.2. B). X-Ray Diffraction Analysis:

The XRD pattern (Fig 7.2 b) displayed sharp diffraction peaks at 2θ values of 32.5°, 35.6°. 38.8°,48.7°,53.5°, 58.3°, 61.6°, 66.2° and 68.1°, which correspond to the crystal planes (110), (111), (202), (112), (113),(022) and (220). These peaks match the standard monoclinic CuO phase (JCPDS card No: 48-1548), confirming the high crystallinity and purity of the nanoparticles without any detectable impurity peaks.

3.1.2. C). UV-Visible Spectroscopic Analysis:

The UV-Vis absorption spectrum of FV CuO nanoparticles, as illustrated in Fig 7.2 c, reveals a prominent absorption peak at approximately 248 nm. This peak signifies the electronic transition within the CuO nanoparticles, thereby affirming their characterization as nanoscale materials.

3.1.2. D). Tauc's Plot

The Tauc's plot (Fig 7.2 d) derived from the UV-Vis spectrum showed a direct band gap energy of 3.77eV, which is higher than that of bulk CuO (1.2-1.9 eV). This blue shift in the band gap is attributed to quantum confinement effects, confirming the nanosized dimensions of the Fioria vitifolia CuO nanoparticles.

3.1.2. E). SEM and EDX

Scanning Electron Microscopy (SEM) Analysis: The surface morphology of the Fioria vitifolia- mediated CuO nanoparticles was examined using Scanning Electron Microscopy (SEM) at different magnifications **(Fig.no: 2).** The micrographs revealed that the synthesized CuO nanoparticles are irregularly spherical to quasi-spherical in shape, forming agglomerated clusters due to the natural capping action of phytochemicals present in the Fioria vitifolia extract. At lower magnification **(Fig.no: 2a),** larger aggregated structures with porous morphology can be observed, indicating the accumulation of nanosized particles. Higher magnification images **(Fig.no: 2 b-d)** confirm that the individual nanoparticles are uniformly distributed with an average particle size in the range of 80-150nm. The zoomed-in image **(Fig.no: 2 c,d)** highlights the nearly spherical morphology and relatively smooth surface of the particles. The agglomeration observed is attributed to hydrogen bonding and van der Waals interactions among particles, as well as the presence of organic residues from plant metabolites acting as stabilizers. These results confirm that the green synthesis route using Fioria vitifolia extract effectively produced nanostructured CuO particles with fine morphology and nanoscale dimensions suitable for biological and catalytic applications.

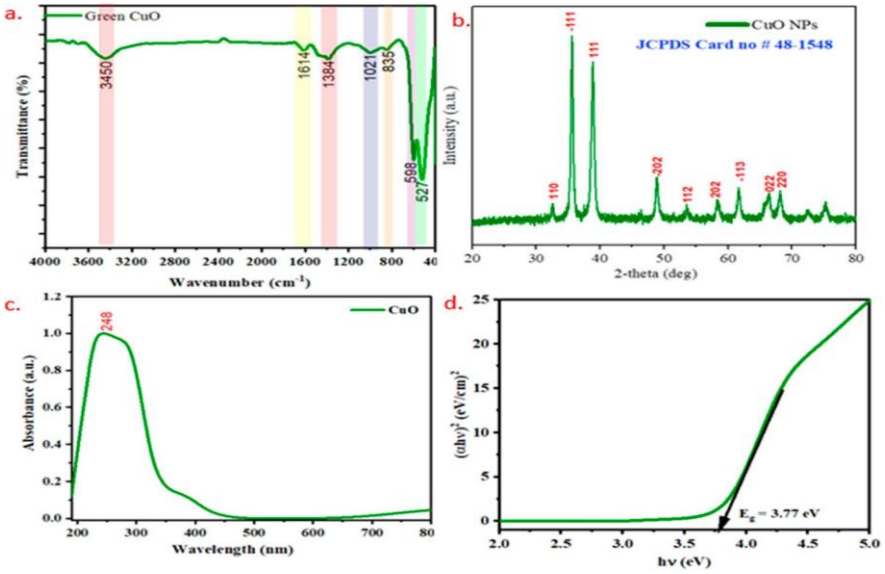

Fig.no: 2. Characterization of FV CuO NPs

2.a) FT-IR Spectrum of Synthesized FV CuO NPs, 2.b) XRD Spectrum of the synthesized FV CuO NPs, 2.c) UV-Vis Spectrum of the synthesized FV CuO NPs and 2.d) Tauc's plot of the synthesized FV CuO NPs

The elemental composition of CuO nanoparticles synthesized using Fioria vitifolia extract was examined through Energy Dispersive X-Ray Spectroscopy (EDX) as illustrated in **(Fig. no: 3 e)**. The resulting spectrum exhibited distinct peaks for copper (Cu) and oxygen (O), confirming the successful formation of copper oxide nanoparticles without any detectable impurities. Notably, the Cu peaks at approximately 1.0 keV (Cu Lα) and 8.0 keV (Cu Kα) were prominent, while the oxygen peaks around 0.5 keV (O Kα) indicated the presence of oxygen in its oxide form. Quantitative analysis indicated that the nanoparticles comprised 3.36 wt% Cu and 36.63 wt% O, translating to 53.94 at% Cu and 46.06 at% O, which closely matches the expected stoichiometric ratio of CuO. The absence of additional elemental signals further supports the conclusion that the synthesized nanoparticles are chemically pure and free from contamination, thereby validating the efficacy of the green synthesis method utilizing FV extract as a natural reducing and stabilizing agent.

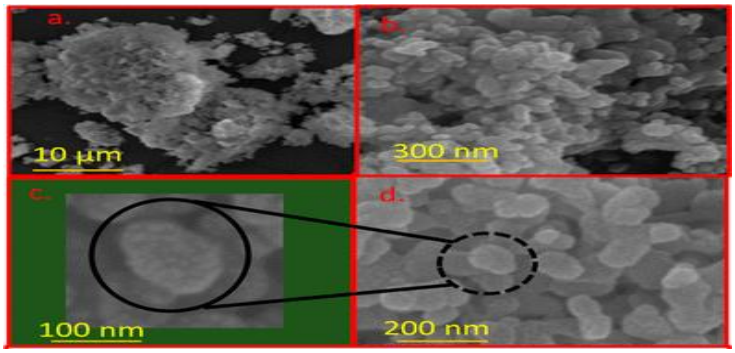

Fig. no: 3. (a-d) SEM micrographs of the Synthesized FV CuO NPs at different magnifications a) aggregated morphology b) uniform Nano sized particles, c, & d) magnified with highlighting spherical CuO nanoparticles structure.

3.1.2. F). Transmission Electron Microscopy:

Transmission Electron Microscopy (TEM) Analysis: TEM micrographs **(Fig. no: 4 and 5)** illustrate the nanoscale morphology and size distribution of FV CuO NPs. The particles appear spherical and uniformly distributed, with sizes ranging between 8-35nm. The inset magnified regions clearly show distinct, well dispersed nanoparticles, confirming their

nanometric dimension. The small particle size and uniform dispersion are attributed to the stabilizing and reducing phytochemicals present in the Fioria vitifolia leaf extract, which efficiently controlled the nucleation and growth of CuO nanoparticles.

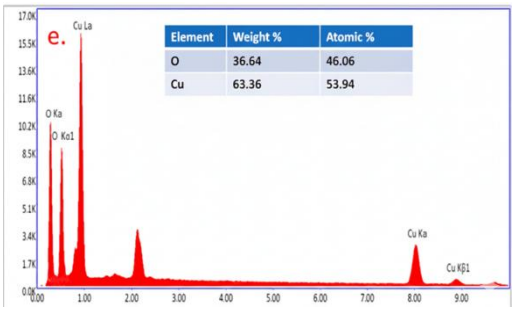

Fig. no: 4. EDX Spectrum of the synthesized FV CuO NPs

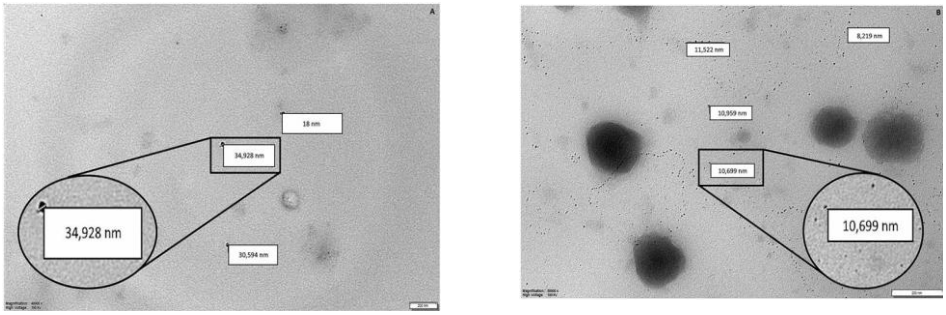

Fig. no: 5. TEM Micrographs of Synthesized FV CuO NPs

3.1.2. G). Zeta potential:

The zeta potential analysis of Fioria vitifolia mediated CuO nanoparticles was carried out at 25°C and the obtained values range from -31.2 mV to -33.8mV, with a mean value of -32.8mV. The negative surface charge indicates that the nanoparticles possess good stability due to electrostatic repulsion between similarly charged particles, which prevents agglomeration in suspension. Generally, nanoparticles with zeta potential values greater than ±30mV are considered stable, confirming that the synthesized CuO nanoparticles exhibit excellent colloidal stability and uniform dispersion in the medium. The result was shown in **(Table no: 1& Fig. no: 6)**

Table no: 1. Zeta Potential of the Synthesized CuO NPs

S.NO	Temperature (°C)	Zeta Potential (mV)
1.	25	-31.2
2.	25	-33.8
3.	25	-33.5
4.	25	-32.8
Mean	25	-32.8

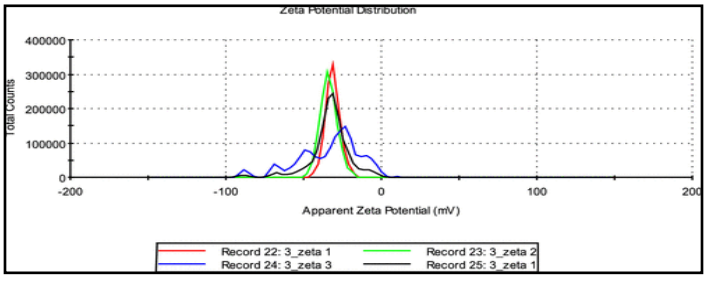

Fig. no: 6. Zeta Potential of the Synthesized CuO NPs

3.1.3. Pharmacological Evaluation of FV mediated CuO NPs:

3.1.3. a. Antioxidant Assayof Fioria vitifolia extract:

DPPH free radical Scavenging Assay:

The antioxidant potential of Fioria vitifolia-mediated CuO nanoarticles was evaluated using the DPPH free radical scavenging assay and compared with the standard ascorbic acid. As shown in the figure 7.8, both samples exhibited a concentration-dependent increase in percentage inhibition of DPPH radicals within the tested range of 20-100µg/ml.

The standard ascorbic acid displayed the highest scavenging activity with an IC 50 value of 39.98µg/ml (r2=0.884), whereas the CuO nanoparticles showed an IC 50 value of 447.5 µg/ml (r2=0.996). Although the antioxidant capacity of CuO NPs was lower than that of ascorbic acid, the gradual enhancement of activity with increasing concentration indicates their effective radical quenching ability. The observed antioxidant potential may be attributed to the presence of bioactive phytoconstituents from the Fioria vitifolia extract acting as capping and stabilizing agents on the nanoparticles surface, facilitating electron donation to neutralize DPPH radicals. The result was shown in **(Table no: 2**& **Fig. no: 7)**

Table no: 2. DPPH free radical Scavenging Assay

S. No	Concentration of Sample (µg/ml)	Inhibition of DPPH (%) Control (Ascorbic acid)	Inhibition of DPPH (%) CuO NPs
1.	20	26.5±1.3	14.3±1.5
2.	40	47.2±1.6	28.4±1.2
3.	60	67.3±1.1	48.3±1.4
4.	80	84.2±1.5	68.1±1.1
5.	100	97.1±2.3	88.5±2.2

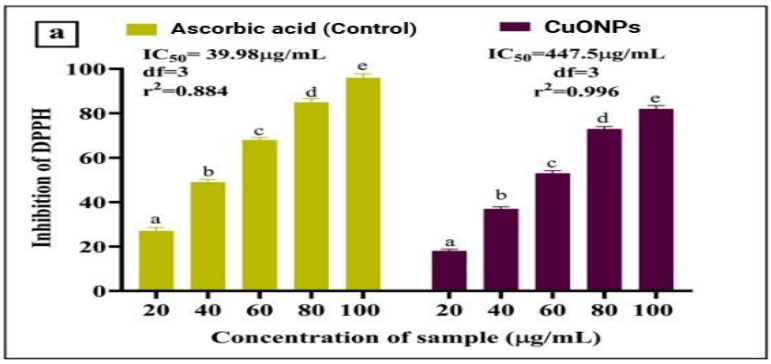

Fig. no: 7. DPPH Free Radical scavenging Assay

ABTS Radical Scavenging Assay:

As depicted in the **figure no: 8**, both the standard and the CuO NPs exhibited concentration-dependent increases in percentage inhibition of ABTS radicals (20-100µg/ml). The synthesized CuO nanoparticles demonstrated a strong radical scavenging capacity with an IC50 value of 207.9µg/ml (r2=0.98) while ascorbic acid showed an IC 50 value of 480.5µg/ml (r2=0.99). Interestingly, the CuO nanoparticles exhibited a comparatively higher antioxidant potential than the standard, suggesting that the Phytochemical compounds from Fioria vitifolia present on the nanoparticles surface may act synergistically to neutralize free radicals. The enhanced activity can also be attributed to the small particle size and large surface area which facilitate efficient electron transfer and hydrogen donation to the ABTS radical species. The result was shown in **(Table no: 3** & **Fig. no: 8)**

Table no: 3. ABTS Radical Scavenging Assay

S.No	Concentration of Sample (µg/ml)	Inhibition of ABTS (%) Control (Ascorbic acid)	Inhibition of ABTS (%) CuONPs
1.	20	22.4±1.2	15.6±1.0
2.	40	42.8±1.5	32.7±1.3
3.	60	63.5±1.8	51.2±1.5
4.	80	84.1±2.1	70.4±1.9
5.	100	98.3±2.4	86.9±2.0

Fig. no: 8. ABTS Radical Scavenging assay

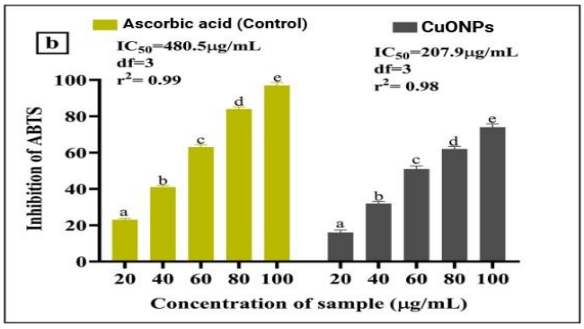

3.1.3. b. In-vitro Anti-inflammatory activity of Fioria vitifolia extract by Protein denaturation assay:

The anti-inflammatory potential of Fioria vitifolia (FV) extract, copper-oxide (CuO) and green synthesized Copper oxide nanoparticles (CuO NPs) was assessed using the protein denaturation inhibition method, as illustrated in **Figure no: 9** and summarized in the **Table no: 4.** Denaturation of proteins is a well-established cause of inflammation, and substances that can inhibit this process are considered to possess anti-inflammatory properties.

At a concentration of 50µg/ml, the standard control showed the highest inhibition of protein denaturation (89.2±2.5%) followed by the CuO samples, which exhibited inhibition ranging from 95.1±2.0% to 88.4±2.5% across concentrations of 25-150µg/ml. The CuO NPs demonstrated a moderate inhibitory effect, decreasing from 80.3±2.8% at 25µg/ml to 66.2±3.0% at 150µg/ml, whereas the FV extract alone showed a comparatively lower inhibition (52.4±3.1%)

The results reveal that both CuO and CuONPs possess notable protein stabilizing properties, indicating effective anti-denaturation potential. The slightly reduced inhibition observed for CuO NPs compared to bulk CuO may be due to the presence of Phytochemical capping agents that modulate the nanoparticles surface reactivity. Nevertheless, the nanoparticles still demonstrated considerable activity, which can be attributed to their small particle size, large surface area and the synergistic influence of bioactive compounds from Fioria vitifolia.

Table no: 4. % Inhibition of Protein Denaturation Assay of Fioria vitifolia extract

Sample	Concentration(µg/ml)	% Inhibition (Mean±SD)
Control	50	89.2±2.5
FV Extract	50	52.4±3.1
CuO	25	95.1±2.0
	50	91.7±2.2
	150	88.4±2.5
CuONPs	25	80.3±2.8
	50	76.5±2.7
	150	66.2±3.0

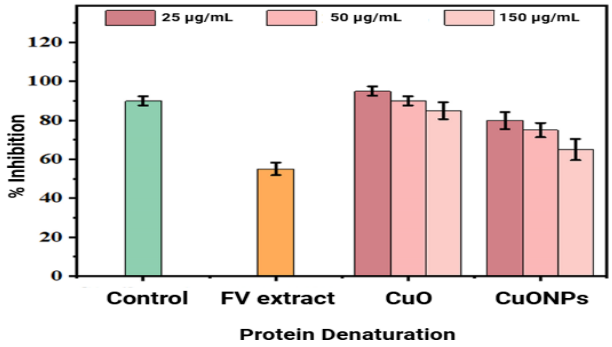

Fig. no: 9. Protein Denaturation Inhibition Assay of Fioria vitifolia extract

3.1.3. b. Antimicrobial Assay:

The antibacterial and antifungal activities of Fioria vitifolia- mediated CuO nanoparticles were evaluated against Pseudomonas aeruginosa, Staphylococcus aureus, Proteus vulgaris, Enterococcus faecalis and Candida albicans.The results demonstrated that all samples exhibited dose-dependent antimicrobial activity. Among the tested samples, S3 showed the highest inhibition zones against all the microorganisms, particularly against P.Aeruginosa (18mm; 82% activity) and S.aureus (13mm; 93% activity), when compared with the standard antibiotic-Amoxicillin. The lower activity observed in p.vulgaris indicates species specific resistance. Over all the findings, the biosynthesized FV CuO NPs possess significant broad-spectrum antimicrobial potential, which increases with concentration and may be attributed to their small size and surface reactivity.

Table no: 5.1. Antimicrobial activity of FV CuO NPs

Samples	S.aureus		P.aeruginosa		P.vulgaris	
	Zone of inhibition (mm)	**% activity Index**	**Zone of inhibition (mm)**	**% activity Index**	**Zone of inhibition (mm)**	**% activity Index**
S1	8	57	8	36	1	13
S2	12	86	16	73	5	63
S3	13	93	18	82	3	38
Antibiotic	14	100	22	100	8	100

Table no: 5.2. Antimicrobial activity of FV CuO NPs

Samples	E.faecalis		C.albicans	
	Zone of Inhibition (mm)	**% Activity Index**	**Zone of Inhibition (mm)**	**% Activity Index**
S1	4	18	7	41
S2	14	64	10	59
S3	16	73	14	82
Antibiotic	22	100	17	100

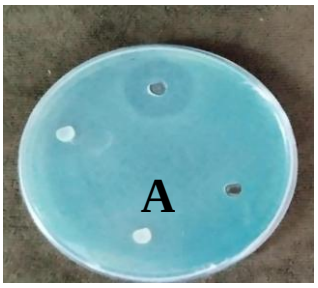

A -Pseudomonas aeruginosa



B - Staphylococcusaureus

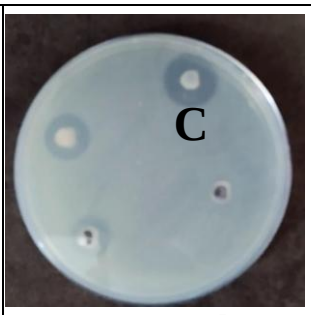

C – Proteus vulgaris

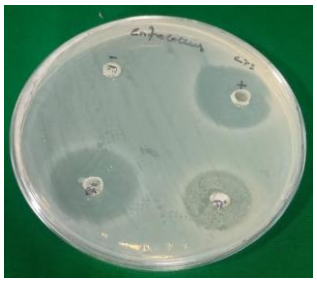

D – Enterococcus faecalis

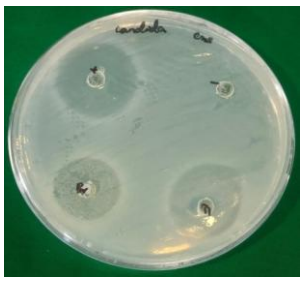

E. Candida albicans

Fig. no: 10. Antibacterial and Antifungal Activity of FV CuO NPs

3.1.3. c. In-vitro studies of Anticancer Assay:

The cytotoxic effects of FV-CuONPs were evaluated on the MDA-MB-231 human breast cancer cell line using the MTT test, with findings compared to the standard treatment of tamoxifen citrate. They both reduced cell viability in a concentration-dependent manner. Tamoxifen citrate and FV-CuONPs had 85.1% and 86.4% viability rates, respectively, at 5 µg/mL concentrations. The life span decreased to 77.1% and 75.1% at 10 µg/mL, and 50.8% and 51.8% at 15 µg/mL. At the maximum concentration of 20 µg/mL, the viability of tamoxifen citrate and FV-CuONPs decreased significantly, with 25.4% and 28.4%, respectively. These findings indicate that FV-CuONPs have significant dose-dependent cytotoxicity, highlighting their potential as an effective therapy for triple-negative breast cancer cells. The result was shown in **Table no: 6 & Fig. no: 11 &12.**

Statistical analysis via one- way ANOVA followed by Dunnett's post hoc test confirmed that reductions in viability were significant at all concentrations tested ($p < 0.05$ to $p < 0.001$). These findings indicate a strong cytotoxic effect of FV-CuO NPs on MDA-MB-231 cells, with the half maximal inhibitory concentration (IC50) likely near 15 µg/ml.

Table no: 6. Effect of FV-CuO NPs on MDA-MB-231 cell morphology and viability

Conc (µg/ml)	STD Temoxifen citrate (µg/ml)	FV-CuONPs
0	100%	100%
5	85.1%	86.4%
10	77.1%	75.1%
15	50.8%**	51.8%**
20	25.4%**	28.4%***

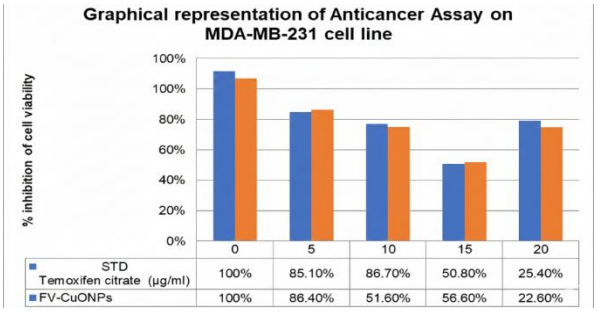

Fig. no: 11. Graphical representation of Anticancer Assay on MDA-MB-231 cell line

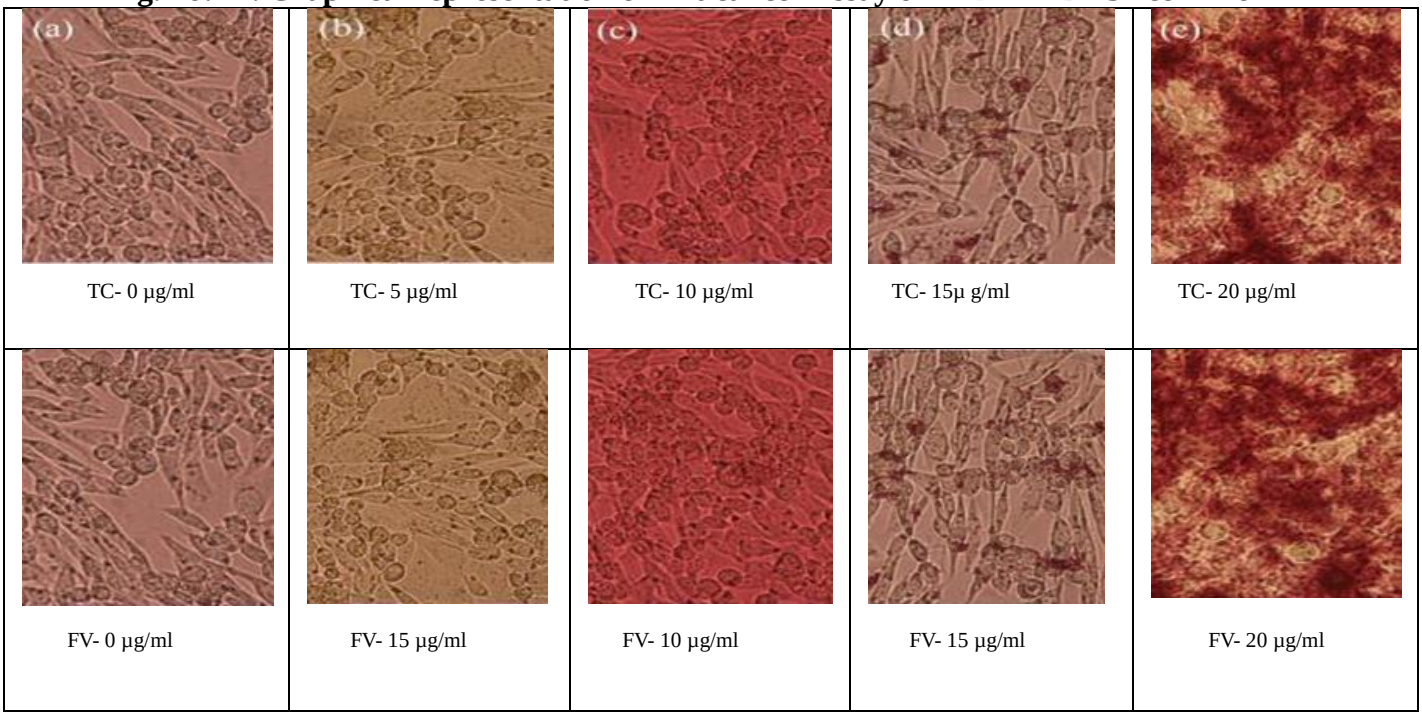

Fig. no: 12. Effect of cell morphology of MDA-MB-231 cell line

3.1.3. d. In-vivo studies in Wistar Rats:

Liver function Tests:

Alanine transaminase Assay ALT (U/L):

The inhibitory effect of FV-CuONPs on alanine transaminase (ALT) levels was assessed and compared with the standard drug, tamoxifen citrate. Both treatments demonstrated a concentration-dependent modulation of ALT enzyme activity, with FV-CuONPs exhibiting inhibition patterns comparable to those of the standard. Statistical analysis indicated no significant difference between the two treatments, suggesting that FV-CuONPs effectively regulate ALT activity. The result was shown in **Table no: 7 & Fig. no: 13.**

Table no: 7. % Inhibition of FV-CuONPs on Alanine transaminase ALT (U/L)

Conc (µg/ml)	STD Temoxifen citrate (µg/ml)	FV-CuONPs
0	38.4±2.1	38.4±2.1
5	80.3±2.4	85.3±3.4
10	55.2±1.0	60.2±2.8
15	50.1±1.9	44.1±1.9
20	48.9±2.4	50.5±2.4

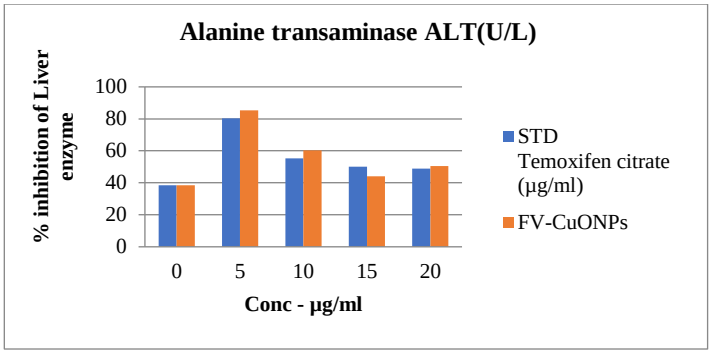

Fig. no: 12. Graphical representation % Inhibition of FV-CuONPs on Alanine transaminase ALT (U/L)

Aspartate aminotransferase Assay AST (U/L):

The inhibitory effects of FV-CuONPs on alanine transaminase (ALT) activity were assessed in relation to the standard treatment, tamoxifen citrate. Both FV-CuONPs and tamoxifen demonstrated a concentration-dependent inhibition of ALT enzyme activity. Notably, FV-CuONPs exhibited a gradual inhibitory effect akin to that of tamoxifen, with increased concentrations leading to more significant reductions in activity. These results suggest that FV-CuONPs are effective in suppressing ALT activity, comparable to the Standard drug. The result was shown in **Table no: 8 & Fig. no: 14.**

Table no: 8. % Inhibition of FV-CuONPs on Aspartate aminotransferase AST (U/L)

Conc (µg/ml)	STD Temoxifen citrate (µg/ml)	FV-CuONPs
0	42.7±1.8	42.7±1.8
5	85.2±3.8	92.6±4.1
10	50.1±2.1**	68.4±3.1***
15	45.2±2.2**	50.2±2.3**
20	39.8±1.0**	57.8±2.9***

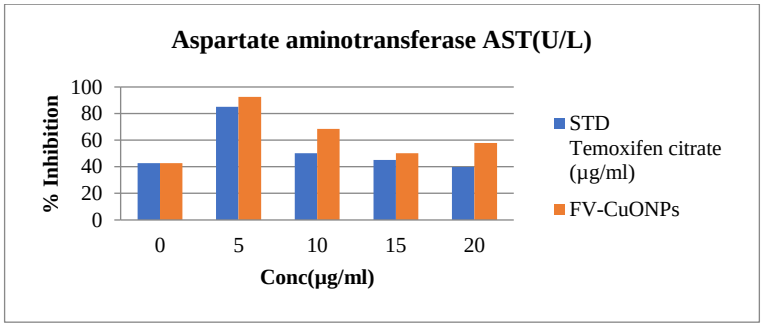

Fig. no: 13. Graphical representation % Inhibition of FV-CuONPs on Aspartate aminotransferase

Alkaline phosphatase ALP (U/L):

The Effect of FV-CuONPs on Alanine Transaminase (ALT) Activity The effect of FV-CuONPs on alanine transaminase (ALT) activity was evaluated and compared to tamoxifen citrate, the standard drug. Both treatments produced a concentration-dependent alteration of ALT enzyme levels. FV-CuONPs blocked enzymes in a process similar to tamoxifen, with higher doses resulting in a significant decrease in ALT activity. The result was shown in **Table no: 9 & Fig. no: 15.**

Table no: 9. % Inhibition of FV-CuONPs on Alkaline phosphatase ALP (U/L)

Conc (µg/ml)	STD Temoxifen citrate (µg/ml)	FV-CuONPs
0	110.5± 5.2	110.5± 5.2
5	197.8±5.7	210.8±6.7
10	141.4±4.9***	150.4±5.5***
15	112.1±3.0**	120.1±4.3**
20	130.7±4.7***	132.7±4.9***

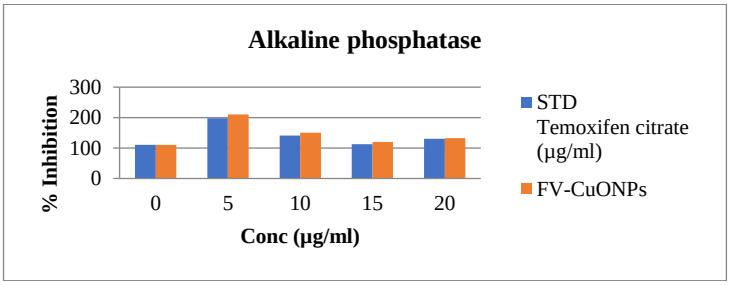

Fig. no: 14. Graphical representation % Inhibition of FV-CuONPs on Alkaline phosphatase

Oxidative parameters analysis:

The evaluation of oxidative parameters showed that after treatment with FV-CuONPs, there were dose-dependent changes in the activity of antioxidant enzymes and oxidative stress indicators. Both catalase (CAT) and superoxide dismutase (SOD) activities significantly decreased at the lowest concentration of 5 µg/ml when compared to the control group. However, these activities gradually increased with higher doses of FV-CuONPs, indicating a partial recovery of the antioxidant defense system. On the other hand, malondialdehyde (MDA) levels declined as the concentration of FV-CuONPs grew, but they were high at the 5 µg/ml concentration, suggesting increased lipid peroxidation. These findings suggest that while greater doses of FV-CuONPs aid in the restoration of antioxidant equilibrium, less amounts cause oxidative stress. The result was shown in **Table no: 10 & Fig. no: 16.**

Table. No: 10. Urine function test of FV-CuONPs

Parameter	Group-1 (Control)	Group-2 FV-CuoNPS-5µg/ml	Group-3 FV-CuoNPS-10µg/ml	Group-4 FV-CuoNPS-15µg/ml	Group-5 FV-CuoNPS-20µg/ml
STD Tamoxifen citrate (µg/ml)	0.6±0.02	1.0±0.09	0.9±0.05**	0.7±0.03**	1.0±0.06*
Bilirubin (mg/dL)	0.7±0.04**	1.9±0.09*	1.2±0.05**	0.8±0.03**	1.0±0.06*
Creatinine (mg/dL)	0.6±0.03**	1.4±0.05**	1.0±0.04***	0.7±0.02**	0.9±0.03**
Urea (mg/dL)	28.3±1.6*	56.7±2.2*	40.4±1.9**	30.1±1.4*	35.5±1.7*
BUN (mg/dL)	13.2±0.7*	27.5±1.2*	20.1±0.9*	15.8±0.6*	17.6±0.8*

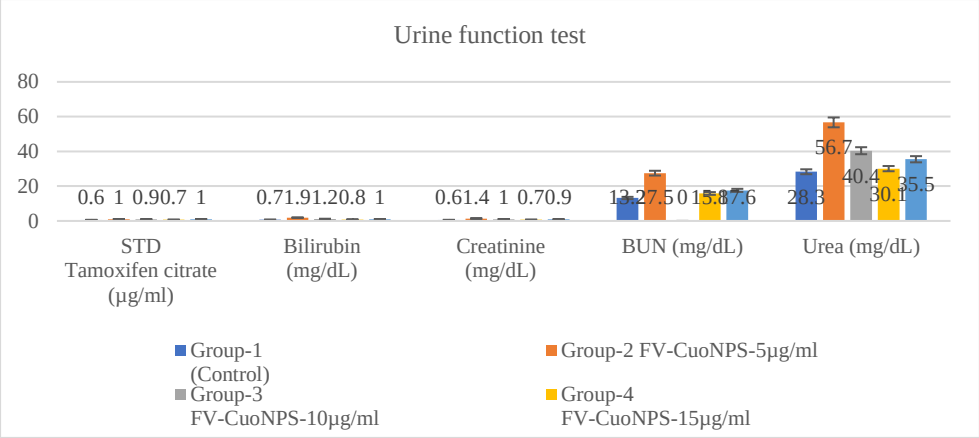

Fig. no: 15. Graphical representation Urine function test of FV-CuONPs

Table. No: 11. Blood Parameters or Haematology

Parameter	Group-1 Control	Group-2 FV-CuoNPS-5µg/ml	Group-3 FV-CuoNPS-10µg/ml	Group-4 FV-CuoNPS-15µg/ml	Group-5 FV-CuoNPS-20µg/ml
RBC(×10⁶/µL)	7.8±0.3	5.4±0.2	6.3±0.3	7.1±0.2	6.8±0.3
WBC (×10³/µL)	8.4±0.4	13.6±0.5	10.8±0.4	9.1±0.3	9.8±0.3
Platelets (×10³/µL)	310±12.1	205±9.8	260±10.2	295±11.5	280±10.9
Hemoglobin (g/dL)	14.5±0.5	9.8±0.3	12.1±0.4	13.6±0.4	12.8±0.3

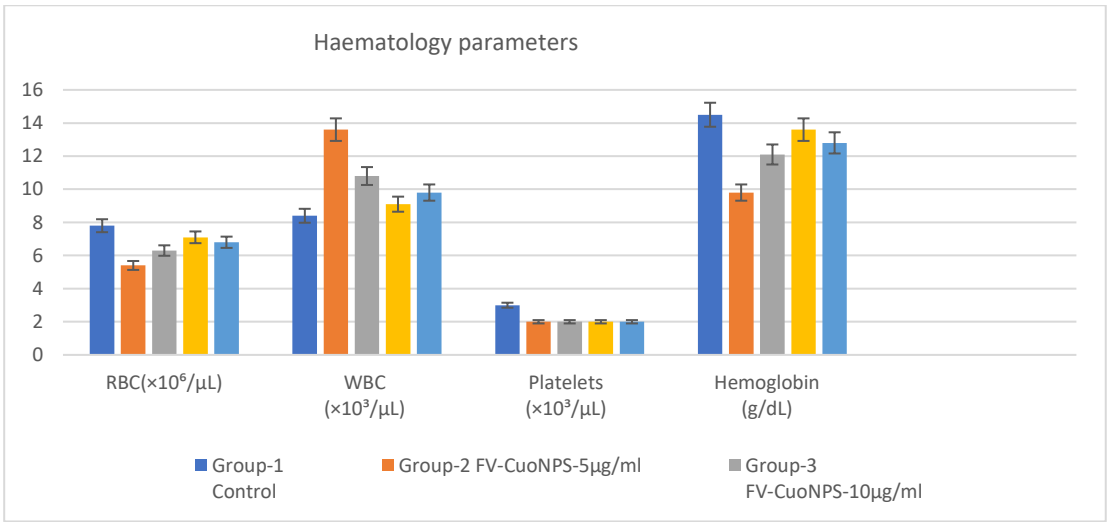

Fig. no: 16. Graphical representation Blood Parameters

Table. No: 12. Estimation of SOD (U/mg protein)

Conc (µg/ml)	STD Temoxifen citrate (µg/ml)	FV-CuONPs
0	15.1±0.7	15.6±0.7
5	6.5±0.3	6.4±0.3
10	9.0±0.4***	10.5±0.4***
15	12.8±0.6**	13.8±0.6**
20	10.9± 0.5***	11.9± 0.5***

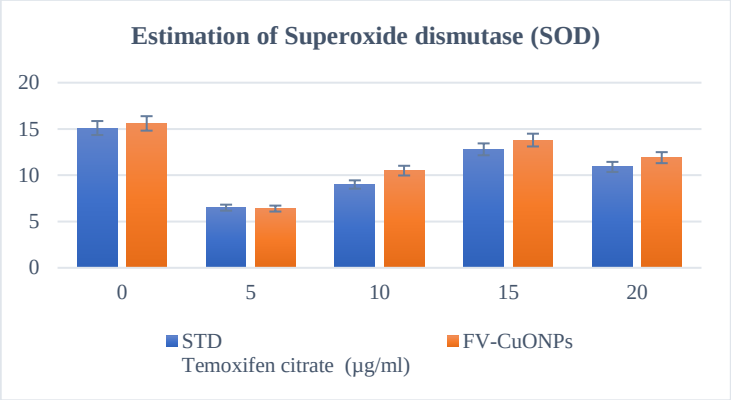

Fig. no: 17. Graphical representation of Estimation of SOD (U/mg protein)

Table. No: 13. Estimation of Catalase (CAT) (U/mg protein)

Conc (µg/ml)	STD Temoxifen citrate (µg/ml)	FV-CuONPs
0	20.3 ± 1.0	22.3 ± 1.0
5	10.1 ± 0.4**	9.1 ± 0.4**
10	17.8 ± 0.6**	15.2 ± 0.6**
15	23.4 ± 0.9**	20.5 ± 0.9**
20	19.1 ± 0.7**	18.4 ± 0.7**

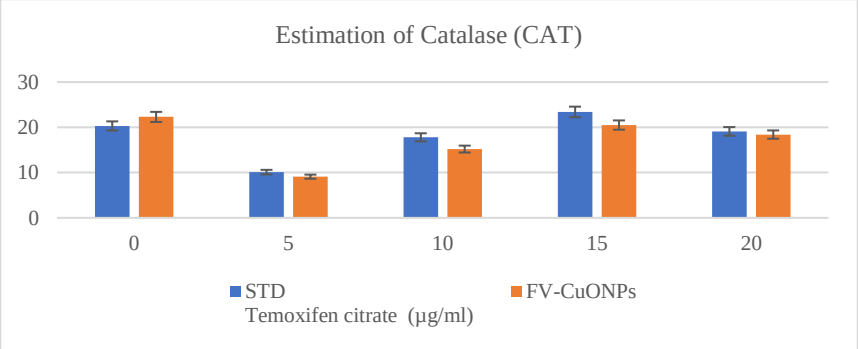

Fig. no: 18. Graphical representation of Estimation of CAT (U/mg protein)

Table. No: 13. Estimation of MDA (Mol/mg protein)

Conc (µg/ml)	STD Temoxifen citrate (µg/ml)	FV-CuONPs
0	1.0 ± 0.05	1.2 ± 0.05
5	2.8 ± 0.13**	3.8 ± 0.15**
10	1.6 ± 0.1**	2.6 ± 0.1**
15	1.2 ± 0.02**	1.5 ± 0.06**
20	1.0 ± 0.04**	1.9 ± 0.08**

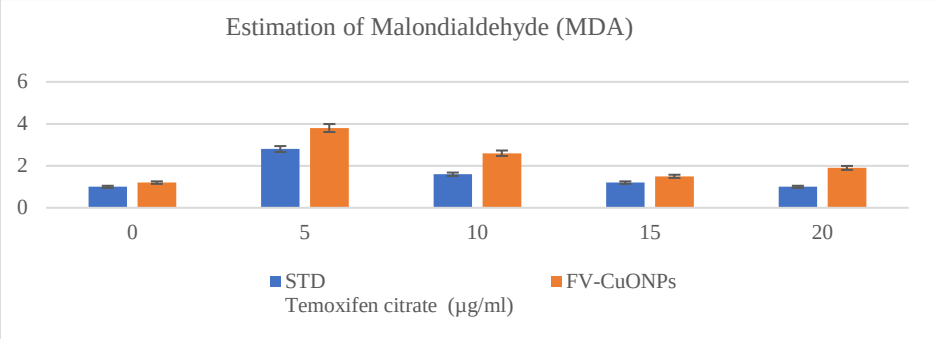

Fig. no: 19. Graphical representation Estimation of CAT (U/mg protein)

Table. No: 14. Estimation of GSH (nmol/mg protein)

Conc (µg/ml)	STD Temoxifen citrate (µg/ml)	FV-CuONPs
0	7.8 ± 0.3	6.8 ± 0.3
5	3.9 ± 0.1	3.1 ± 0.1**
10	4.2 ± 0.2**	4.9 ± 0.2**
15	8.1 ± 0.3**	6.1 ± 0.2**
20	6.6 ± 0.2**	5.6 ± 0.2**

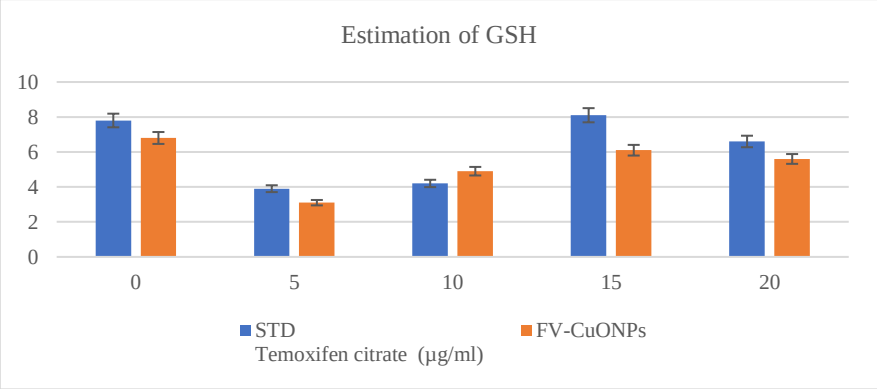

Fig. no: 20. Graphical representation Estimation of GSH (U/mg protein)

Histopathology Studies:

Histopathology of Liver:

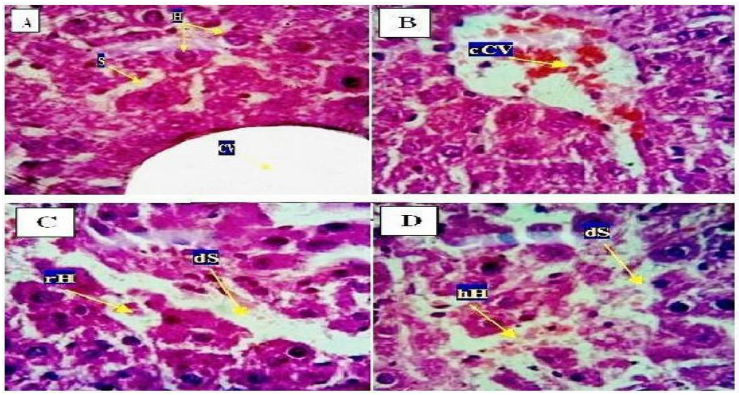

Fig. no: 21. Histopathology of Liver

- Group A (**Control**) showed normal hepatic architecture characterized by a clearly defined central vein (CV), regular sinusoidal spaces (S), and healthy hepatocytes (H).
- Group B (**Toxin-Treated Group**) exhibited marked liver damage, including a congested central vein (cCV), prominent cellular infiltration, and areas of necrosis.

- Group C (**Treatment with FV extract**) demonstrated noticeable improvement, with regenerated hepatocytes (rH) and reduced sinusoidal dilation (dS).
- Group D (**Treatment with FV CuO NPs**) showed significant healing effects, evidenced by the presence of healing hepatocytes (hH), improved overall liver structure, and minimal sinusoidal dilation (dS).

Histopathology of Kidney:

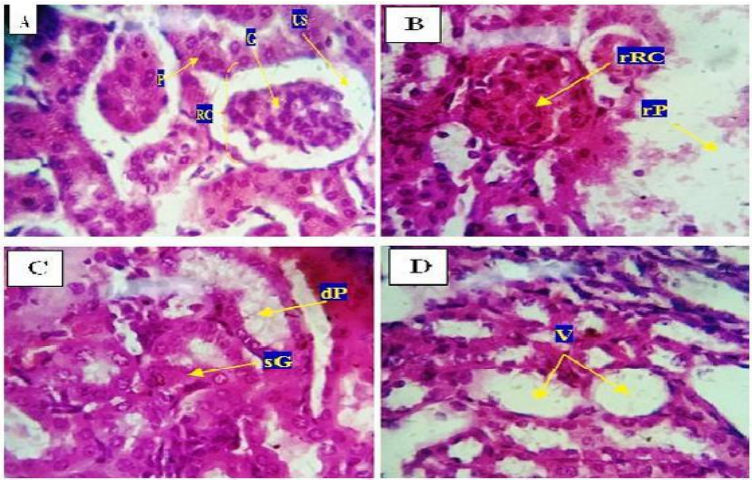

Fig. no: 22. Histopathology of Kidney

- Group A (**Control Group**) exhibited normal renal histology, characterized by an intact renal corpuscle (RC), well-defined proximal (P) and distal convoluted tubules (C), a clear urinary space (US), and a healthy glomerulus (G).
- Group B (**Toxin-Treated Group**) showed signs of renal injury, including a regenerated renal corpuscle (rRC), reduced proximal tubule function (rP), and mild glomerular damage.
- Group C (**FV Extract Treated Group**) displayed slight glomerular shrinkage (sG) along with evidence of a disrupted proximal tubule (dP), indicating moderate renal alterations.
- Group D (**CuO NPs Treated Group**) presented visible vacuolation (V), mild cellular swelling, and retained near-normal renal architecture, suggesting partial protective or restorative effects.

3.2. Discussion:

The percentage yield of Fioria vitifolia leaf extract was determined using 80% Ethanol as the solvent. The extraction yielded a viscous, dark brownish-green colour, indicating the presence of a high concentration of phytoconstituents. The yield is 8.95%.

The preliminary phytochemical studies were done in the Ethanolic extraction of Fioria vitifolia leaves showed the presence of Alkaloids, Tannins, saponins Triterpenoids, Flavanoids, Proteins, Phenolic Compounds in high concentration. Glycosides, carbohydrates were present in low concentration. Steroids was very low in concentration or not present.

The FT-IR spectroscopic Analysis revealed distinct absorption peaks corresponding to various functional groups involved in nanoparticles formation and stabilization. The characteristic bands appearing below 600cm -1, particularly at 598 and 527 cm-1, confirm the CuO stretching vibrations, validating the successful formation of copper oxide nanoparticles. These findings indicate that bioactive compounds present in the Fioria vitifolia extract played a dual role as both reducing and stabilizing agents in the eco-friendly synthesis of FV CuO NPs.

The XRD pattern confirmed the high crystallinity and purity of the nanoparticles without any detectable impurity peaks. FV CuO NPs, indicating the electronic transition of CuO nanoparticles and confirming their nanoscale nature.

Tauc's Plot represented the band gap is attributed to quantum confinement effects, confirmed the nanosized dimensions of the Fioria vitifolia CuO nanoparticles.

SEM confirmed that the green synthesis route using Fioria vitifolia extract effectively produced nanostructured CuO particles with fine morphology and nanoscale dimensions suitable for biological and catalytic applications.

EDX suggested that the synthesized nanoparticles are chemically pure and free from contamination. These results confirms the successful green synthesis of CuO nanoparticles using FV extract as a natural reducing and stabilizing agent, confirming their purity and elemental composition.

TEM confirmed the small particle size and uniform dispersion are attributed to the stabilizing and reducing phytochemicals present in the Fioria vitifolia leaf extract, which efficiently controlled the nucleation and growth of CuO nanoparticles.

Zeta potential confirmed the synthesized CuO nanoparticles exhibit excellent colloidal stability and uniform dispersion in the medium.

Antimicrobial Assay studies confirmed the antibacterial and antifungal activity possessed significant broad-spectrum activity.

Antioxidant Activity assayed by DPPH Free Radical Scavenging Assay and ABTS radical scavenging assay. This test confirmed that the phytochemical compounds from Fioria vitifolia present on the nanoparticles surface may act synergistically to neutralize free radicals. The enhanced activity can also be attributed to the small particle size and large surface area which facilitate efficient antioxidant activity.

An anti-inflammatory assay result revealed that both CuO and CuONPs possess notable protein stabilizing properties, indicating effective anti-denaturation potential.

The anticancer activity of Untreated Control cells exhibited normal spindle- shaped morphology with strong adherence. Cells treated with 5µg/ml FV-CuONPs displayed mild rounding and reduced confluency. At 10 µg/ml, more pronounced morphological alterations were evident, including cell shrinkage and detachment. Treatment with 15 µg/ml and 20 µg/ml resulted in severe deformation, loss of adhesion and significant cell death, indicative of cytotoxic effects.

FV-CuO nanoparticles (FV-CuONPs) showed strong biochemical and histological protective effects comparable to the standard drug tamoxifen. Enzyme assays revealed that FV-CuONPs produced a concentration-dependent inhibition of ALT, AST, and ALP activities, with no significant difference from the standard drug, indicating effective regulation of liver enzymes. Oxidative stress analysis showed that low doses initially increased oxidative stress, while higher doses improved antioxidant enzyme activity (CAT, SOD) and reduced lipid peroxidation (MDA), suggesting dose-dependent restoration of oxidative balance. Histopathological studies supported the biochemical findings: toxin-treated groups showed clear liver and kidney damage, whereas treatment with FV extract and especially FV-CuONPs promoted tissue healing. FV-CuONPs restored liver structure with healthy hepatocytes and reduced sinusoidal dilation, and improved kidney architecture with minimal swelling and near-normal tubule and glomerular structure. Overall, FV-CuONPs demonstrated potent hepatoprotective and renoprotective effects.

4. CONCLUSION:

The study successfully demonstrated the green synthesis of crystalline and pure copper oxide nanoparticles (CuO NPs) using Fioria vitifolia leaf extract as a natural reducing and stabilizing agent, leveraging the extract's rich profile of phytochemicals (e.g., flavonoids, phenolics). Comprehensive analysis confirmed the nanoscale dimensions, morphology, elemental purity, and excellent colloidal stability of the synthesized CuO NPs. Crucially, these FV-CuO NPs exhibited significant therapeutic properties, including antioxidant, antimicrobial, and anti-inflammatory activities. Furthermore, they showed potent dose-dependent cytotoxic (anticancer) effects against MDA-MB-231 breast cancer cells (a triple-

negative breast cancer line).Overall, the research establishes the biocompatibility and promising therapeutic potential of the F. vitifolia-mediated green synthesized CuO NPs.

5. CONFLICT OF INTEREST:

The authors declare no conflict of interest.

6. ACKNOWLEDGMENTS:

The authors express gratitude to the Pharmacology research facilities in department of pharmacology, JKKMMRF's Annai JKK Sampoorani ammal College of Pharmacy, Komarapalayam, Namakkal (D.t), Tamilnadu, India. For providing experimental support and to the technical staff for their guidance and animal handling.

7. REFERENCE:

1. Farnsworth NR. Ethnopharmacology and drug development. InCiba Foundation Symposium 185-Ethnobotany and the Search for New Drugs: Ethnobotany and the Search for New Drugs: Ciba Foundation Symposium 185 2007 Sep 28 (pp. 42-59). Chichester, UK: John Wiley & Sons, Ltd.
2. Harborne AJ. Phytochemical methods a guide to modern techniques of plant analysis. Springer science & business media; 1998 Apr 30.
3. Kumar S, Pandey AK. Chemistry and biological activities of flavonoids: an overview. The scientific world journal. 2013; 2013(1):162750.
4. World Health Organization. WHO traditional medicine strategy: 2014-2023. World Health Organization; 2013.
5. Dena AS, Abdelaziz OA, El-Sherbiny IM. Nanomaterials: classification, composition, and recent advances in synthesis. Immunomodulatory Effects of Nanomaterials. 2022 Jan 1:1-9.
6. Vincent J, Lau KS, Evyan YC, Chin SX, Sillanpää M, Chia CH. Biogenic synthesis of copper-based nanomaterials using plant extracts and their applications: current and future directions. Nanomaterials. 2022 Sep 23; 12(19):3312.
7. Islam MA, Jacob MV, Antunes E. A critical review on silver nanoparticles: From synthesis and applications to its mitigation through low-cost adsorption by biochar. Journal of Environmental Management. 2021 Mar 1; 281:111918.
8. Dubey SP, Lahtinen M, Sillanpää M. Green synthesis and characterizations of silver and gold nanoparticles using leaf extract of Rosa rugosa. Colloids and Surfaces A: Physicochemical and Engineering Aspects. 2010 Jul 20; 364(1-3):34-41.
9. Dubey SP, Lahtinen M, Sillanpää M. Tansy fruit mediated greener synthesis of silver and gold nanoparticles. Process Biochemistry. 2010 Jul 1; 45(7):1065-71.
10. Jadoun S, Arif R, Jangid NK, Meena RK. Green synthesis of nanoparticles using plant extracts: A review. Environmental Chemistry Letters. 2021 Feb; 19(1):355-74.
11. Azri FA, Selamat J, Sukor R, Yusof NA, Ahmad Raston NH, Nordin N, Jambari NN. Etlingeraelatior-mediated synthesis of gold nanoparticles and their application as electrochemical current enhancer. Molecules. 2019 Aug 29; 24(17):3141.
12. Pal G, Rai P, Pandey A. Green synthesis of nanoparticles: A greener approach for a cleaner future. InGreen synthesis, characterization and applications of nanoparticles 2019 Jan 1 (pp. 1-26). Elsevier.
13. Alhalili Z. Green synthesis of copper oxide nanoparticles CuO NPs from Eucalyptus Globoulus leaf extract: Adsorption and design of experiments. Arabian Journal of Chemistry. 2022 May 1; 15(5):103739.
14. Said MI, Othman AA. Structural, optical and photocatalytic properties of mesoporous CuO nanoparticles with tunable size and different morphologies. RSC advances. 2021; 11(60):37801-13.
15. Aroob S, Carabineiro SA, Taj MB, Bibi I, Raheel A, Javed T, Yahya R, Alelwani W, Verpoort F, Kamwilaisak K, Al-Farraj S. Green synthesis and photocatalytic dye degradation activity of CuO nanoparticles. Catalysts. 2023 Feb 28;13(3):502.
16. Mobarak MB, Sikder MF, Muntaha KS, Islam S, Rabbi SF, Chowdhury F. Plant extract-mediated green-synthesized CuO nanoparticles for environmental and microbial remediation: a review covering basic understandings to mechanistic study. Nanoscale Advances. 2025; 7(9):2418-45.
17. https://en.wikipedia.org/wiki/Hibiscus_vitifolius.
18. Kundu BC, Biswas C. On Fioriavitifolia (L.) Mattei. Nelumbo. 1974:125-38.
19. Mahalakshmi K, Senthilkumar N, Solairaj P, Parthiban KG. Isolation of triterpenes from Fioriavitifolia (L.) and its antioxidant activity.
20. Mahalakshmi K, Natesan SK, ganesanParthiban K, Sekar G. Anti-inflammatory and antipyretic activity of Fioriavitifolia. International Current Pharmaceutical Journal. 2013 Jun 1; 2(7):119-21.
21. Imath M, Ragavendran C, Kamaraj C, Alrefaei AF, Almutairi MH, Raj M, Rajendran R, Paneerselvam T, Arasu T, Martin TM, Sundaram M. Fioriavitifolia-mediated silver nanoparticles: Eco-friendly synthesis and biomedical potential. Journal of Water Process Engineering. 2024 Sep 1; 66:106020.

22. Imath M, Ragavendran C, Kamaraj C, Raja RK. Eco-friendly synthesis of chitosan NPs from Fioriavitifolia (L.) L: Potential to antibacterial, antioxidant, cytotoxicity properties of HepG2 cells and their evaluation of safety on Zebrafish embryo. Results in Engineering. 2025 Mar 1; 25:104076.
23. López-Bascón MA, De Castro ML. Soxhlet extraction. InLiquid-phase extraction 2020 Jan 1 (pp. 327-354). Elsevier.
24. David J. Newman, Gordon M. Cragg and Kenneth M. Snader. Natural Products as Sources of New Drugs over the Period 1981-2002. J. Nat. Prod. 2003; 66:1022-1037.
25. Meena R, Nandhini A, Kumar P, et al. Fioria vitifolia Linn leaf extract-derived ZnO nanoparticles: green synthesis, characterization and biological activities. Biomass Convers Biorefin. 2024; 14:31687–31702.
26. Sharma P, Urfan M, Anand R. Green synthesis of ZnO nanoparticles using Eucalyptus lanceolata leaf litter. Physiol Mol Biol Plants. 2022; 28:363–381.
27. Kiani D, Wachs IE, Banares MA. X-ray diffraction (XRD). In: Springer Handbook of Advanced Catalyst Characterization. 2023. p. 519–539.
28. Makula P, Pacia M, Macyk W. Determining band gap energy of semiconductor photocatalysts from UV–Vis spectra. J Phys Chem Lett. 2018; 9:6814–6817.
29. Kumar R, et al. Polymer precursor method for the synthesis of zinc oxide nanoparticles: a novel approach. J Mater Sci Nanotechnol. 2023; 24139.
30. Bhuyan T, et al. Biosynthesis of ZnO nanoparticles from Azadirachta indica for antibacterial and photocatalytic applications. Mater Sci Semicond Process. 2015; 32:55–61.
31. Aisida SO, et al. Green synthesis of copper oxide nanoparticles using plant extract and their antimicrobial activities. Sci Rep. 2020; 10:1115.
32. RajeshKumar S, Bharath LV. Mechanism of plant-mediated synthesis of silver nanoparticles – a review. Chem Biol Interact. 2017; 273:219–227.
33. Rani P, Rajasekaran R. Green synthesis and characterization of copper oxide nanoparticles using Coleus aromaticus leaf extract. Int J Nanosci Nanotechnol. 2018; 14(2):111–119.
34. Brand-Williams W, Cuvelier ME, Berset C. Use of a free radical method to evaluate antioxidant activity. LWT-Food Sci Technol. 1995; 28:25–30.
35. Flogel A, et al. Comparison of ABTS/DPPH assays to measure antioxidant capacity in foods. J Food Compos Anal. 2011; 24(7):1043–1048.
36. Pellegrini N, et al. Antioxidant activity applying an improved ABTS radical cation decolorization assay. Free Radical Biol Med. 1999; 26:1231–1237.
37. Kumar B, et al. Green synthesis of silver nanoparticles using Andean blackberry fruit extract and evaluation of antimicrobial and anti-inflammatory activity. Asian Pac J Trop Biomed. 2017; 7(9):806–813.
38. Santhoshkumar J, Kumar SV, Rajeshkumar S. Synthesis of ZnO nanoparticles using plant leaf extract against urinary tract infection pathogens. Resour-Effic Technol. 2017; 3(4):459–465.
39. Perumal G, et al. LDPE/PCL nanofibers embedded chlorhexidine diacetate for antimicrobial applications. Mater Today Commun. 2024; 38:107652.
40. Siddiquah A, et al. Green synthesis of silver nanoparticles using plant extract and cytotoxicity evaluation against MDA-MB-231 cell line. Nanomaterials. 2018; 8(6):406.